Chemical acetylation of mitochondrial transcription factor A occurs on specific lysine residues and affects its ability to change global DNA topology

方, 圓

Mitochondrion 53 (2020) 99–108

Contents lists available at ScienceDirect

Mitochondrion

journal homepage: www.elsevier.com/locate/mito

Chemical acetylation of mitochondrial transcription factor A occurs on specific lysine residues and affects its ability to change global DNA topology

Yuan Fang[a], Masaru Akimoto[a,b], Kouta Mayanagi[c], Atsushi Hatano[d], Masaki Matsumoto[d], Shigeru Matsuda[a], Takehiro Yasukawa[a,*], Dongchon Kang[a]

[a] Department of Clinical Chemistry and Laboratory Medicine, Graduate School of Medical Sciences, Kyushu University, 3-1-1 Maidashi, Higashi-ku, Fukuoka-shi, Fukuoka 812-8582, Japan
[b] Department of Clinical Chemistry and Laboratory Medicine, Kyushu University Hospital, 3-1-1 Maidashi, Higashi-ku, Fukuoka-shi, Fukuoka 812-8582, Japan
[c] Medical Institute of Bioregulation, Kyushu University, 3-1-1 Maidashi, Higashi-ku, Fukuoka-shi, Fukuoka 812-8582, Japan
[d] Department of Omics and Systems Biology, Graduate School of Medical and Dental Sciences, Niigata University, 757 Ichibancho, Asahimachi-dori, Chuo-ku, Niigata-shi, Niigata 951-8510, Japan

ARTICLE INFO

Keywords:
TFAM
mtDNA
Mitochondria
Acetylation
Topology

ABSTRACT

Chemical acetylation is postulated to occur in mitochondria. Mitochondrial transcription factor A (TFAM or mtTFA), a mitochondrial transcription initiation factor as well as the major mitochondrial nucleoid protein coating the entire mitochondrial genome, is proposed to be acetylated in animals and cultured cells. This study investigated the properties of human TFAM, in conjunction with the mechanism and effects of TFAM acetylation *in vitro*. Using highly purified recombinant human TFAM and 3 kb circular DNA as a downsized mtDNA model, we studied how the global TFAM–DNA interaction is affected/regulated by the quantitative TFAM–DNA relationship and TFAM acetylation. Results showed that the TFAM–DNA ratio strictly affects the TFAM property to unwind circular DNA in the presence of topoisomerase I. Mass spectrometry analysis showed that *in vitro* chemical acetylation of TFAM with acetyl-coenzyme A occurs preferentially on specific lysine residues, including those reported to be acetylated in exogenously expressed TFAM in cultured human cells, indicating that chemical acetylation plays a crucial role in TFAM acetylation in mitochondria. Intriguingly, the modification significantly decreased TFAM's DNA-unwinding ability, while its DNA-binding ability was largely unaffected. Altogether, we propose TFAM is chemically acetylated *in vivo*, which could change mitochondrial DNA topology, leading to copy number and gene expression modulation.

1. Introduction

Protein acetylation is a post-translational modification of lysine residues by which diverse biological processes are regulated (Choudhary et al., 2014). It occurs with donation of an acetyl group of acetyl-coenzyme A (acetyl-CoA) to the ε-amino group of a lysine residue, and neutralizes the positive charge of the ε-amino group and increases steric hindrance of the side chain. Effects of acetylation include changes in nucleic acid binding, protein–protein interaction, and enzymatic activity of the target proteins (Choudhary et al., 2014). A well-known example is histone acetylation that regulates chromatin compaction and transcription, and enzymes with opposing activities (lysine acetyltransferases and lysine deacetylases) are present in the nucleus (Gong and Miller, 2013). Curiously, studies on lysine acetylation have shown that this modification is pervasive in mitochondria: > 60% of mitochondrial proteins contain acetylation sites in mice, and a comparable number of acetylation sites is found in human cell lines (Baeza et al., 2016). While an NAD^+-dependent sirtuin-type deacetylase, SIRT3, regulates the acetylation status of a certain proportion of mitochondrial proteins (Baeza et al., 2016; Hebert et al., 2013; Wagner and Hirschey, 2014), the acetylation mechanism is elusive in mitochondria. Depletion of general control of amino acid synthesis 5-like 1 (GCN5L1) moderately decreased mitochondrial protein acetylation (Scott et al., 2018; Scott et al., 2012), suggesting an involvement of GCN5L1 in the modification. Acetyl-CoA acetyltransferase 1 (ACAT1) was reported to acetylate two mitochondrial

Abbreviations: TFAM, mitochondrial transcription factor A; acetyl-CoA, acetyl-coenzyme A; GCN5L1, general control of amino acid synthesis 5-like 1; ACAT1, acetyl-CoA acetyltransferase 1; mtDNA, mitochondrial DNA; LSP, light-strand promoter; HSP, heavy-strand promoter; HMG, high mobility group; EMSA, electrophoretic mobility shift assay; TCA, tricarboxylic acid

* Corresponding author.
E-mail address: ytakehir@cclm.med.kyushu-u.ac.jp (T. Yasukawa).

https://doi.org/10.1016/j.mito.2020.05.003
Received 27 February 2020; Received in revised form 8 May 2020; Accepted 14 May 2020
Available online 18 May 2020

metabolic proteins (Fan et al., 2014), but whether ACAT1 is responsible for acetylation of other numerous mitochondrial proteins is still unclear. In addition, MOF, a nuclear MYST family acetyltransferase, was reported to be imported in mitochondria (Chatterjee et al., 2016), but whether it acetylates any protein in the mitochondrial matrix is unknown. While GCN5L1 and ACAT1 appear to have roles in mitochondrial protein acetylation, chemical (nonenzymatic) acetylation is postulated to be a plausible source of acetylation in mitochondria (Baeza et al., 2016; Hosp et al., 2017; Wagner and Hirschey, 2014). Inside mitochondria, the pH is considered ~8.0 (Casey et al., 2010) and the concentration of acetyl-CoA is suggested to be 0.1–1.5 mM (Wagner and Payne, 2013); these are sufficient conditions to induce nonenzymatic protein acetylation *in vitro* (Wagner and Payne, 2013).

Mitochondria contain their own genome, the mitochondrial DNA (mtDNA). Mammalian mtDNA is a multicopy circular molecule of ~16.5 kbp, encoding 13 subunits of the oxidative phosphorylation complexes and 22 transfer RNAs and 2 ribosomal RNAs for translating the subunits inside mitochondria (Yasukawa and Kang, 2018). Mitochondrial transcription factor A, TFAM, was originally named after stimulatory activities of mitochondrial transcription initiation (Fisher and Clayton, 1988), and is one of the three components of mitochondrial transcription initiation complexes (the other two being mitochondrial RNA polymerase and mitochondrial transcription factor B2). TFAM binds upstream of the light- and heavy-strand promotors (LSP and HSP) on mtDNA to initiate transcription initiation (Gustafsson et al., 2016). TFAM plays another crucial role with its sequence-nonspecific DNA-binding ability. It was shown that TFAM expression levels are sufficient to coat the mitochondrial genome entirely (Kukat et al., 2011; Takamatsu et al., 2002). Studies on TFAM function in cultured cells (Kanki et al., 2004) and transgenic mice (Ekstrand et al., 2004) have shown that TFAM has an ability to maintain mtDNA, which is distinct from its role as a transcription initiation factor. This view was corroborated by the reports that showed that TFAM binds to almost whole mtDNA regions (Ohgaki et al., 2007; Wang et al., 2013). Currently, TFAM is generally considered the major and sole architectural protein component of the mammalian mitochondrial nucleoid (Farge and Falkenberg, 2019; Kang et al., 2007). High-resolution microscopic studies proposed that the antibody-decorated nucleoid is ~100 nm in size and that a copy of mtDNA is frequently present in each nucleoid (Kukat et al., 2015; Kukat et al., 2011). Therefore, mammalian mtDNA, which is about ~5 μm long, must be extensively folded in the nucleoid. TFAM introduces a 180° U-turn to DNA through DNA bending by the two high-mobility group (HMG)-box domains (HMG-box A and HMG-box B). DNA distortion was shown to occur similarly to the double-stranded DNA (dsDNA) oligonucleotides having LSP and HSP binding site sequences as well as to those with unspecific sequence (Ngo et al., 2014), and the sequence-nonspecific U-turn is considered an important factor for mtDNA packaging. In addition to the U-turn introduction to the DNA backbone, it was proposed that dimerization of DNA-bound TFAM is required for full mtDNA compaction (Ngo et al., 2014) and that local base-pair melting upon TFAM patch formation through corporative TFAM binding (Farge et al., 2012) and DNA looping and cross-strand binding of TFAM (Kaufman et al., 2007; Kukat et al., 2015) contribute to mtDNA compaction.

A previous report showed that increasing TFAM concentration can block replication and transcription in *in vitro* assays, suggesting that the TFAM density on mtDNA molecules regulates the fate of the molecules *in vivo* (Farge et al., 2014), whether they will be used for transcription/replication or maintained silently. This idea is consistent with the results that excessive TFAM overexpression appears to decrease mtDNA replication and transcription in cultured human and *Drosophila* cells (Matsushima et al., 2010; Pohjoismäki et al., 2006). While the quantitative aspect of TFAM is important in mtDNA maintenance and expression, it might not be the sole determinant of such vital processes, as post-translational modifications, acetylation (Dinardo et al., 2003; Hebert et al., 2013; King et al., 2018), phosphorylation (King et al., 2018; Lu et al., 2013; Wang et al., 2014), and *O*-linked β-*N*-acetylglucosamine glycosylation (Suarez et al., 2008), were proposed to play regulatory roles in TFAM function.

The pervasive nature of mitochondrial protein acetylation and the central roles of TFAM in mtDNA maintenance and expression prompted us to examine the possibility of chemical acetylation of TFAM and the influence of this modification on its function. While single-molecule experiments (Farge et al., 2014; King et al., 2018) and crystallography (Ngo et al., 2011; Ngo et al., 2014; Rubio-Cosials et al., 2011) have provided fine-detail information, we used *en-masse* experiment settings with highly purified recombinant human TFAM and 3 kb plasmid DNA as a downsized mtDNA model to study how the global TFAM–DNA interaction is affected/regulated by the quantitative TFAM–DNA relationship and TFAM acetylation.

2. Results

2.1. hTFAM unwinds DNA in the presence of eukaryotic topoisomerase I in a strictly hTFAM–DNA-ratio-dependent manner

Recombinant human TFAM proteins fused with a short polypeptide containing the His tag at the N-terminus, which mimics the native mature form (hereafter called hTFAM), were expressed in *E. coli* and purified extensively by three sequential column chromatography processes to eliminate nuclease contamination (Supplementary Fig. 1A; also see Section 4.1.).

To characterize the DNA-binding ability of hTFAM, we conducted an electrophoretic mobility shift assay (EMSA). hTFAM with increasing concentrations was incubated with 3 kb linear DNA fragments, and the reaction mixtures were directly electrophoresed in agarose gel, followed by DNA visualization with Sybr Green I staining. The hTFAM–DNA fragment molecular ratio at each hTFAM concentration was 1 hTFAM molecule per 56.5, 22.6, 11.3, 7.5, 5.6, 4.5, 3.8, 3.2, and 2.8 bp of DNA fragments. From 1 hTFAM/56.5 bp to 1 hTFAM/5.6 bp, band retardation occurred gradually, and at 1 hTFAM/4.5 bp, the DNA band appeared to show an abrupt upper shift, indicating specific changes in the hTFAM status in terms of DNA interaction (Fig. 1A,B).

Next, we analyzed hTFAM's ability to change DNA topology using an *in vitro* DNA-unwinding assay (Ohgaki et al., 2007). In the presence of eukaryotic (calf thymus) topoisomerase I, we incubated hTFAM with circular 3 kb plasmid DNA that was converted into an open circular form in advance using topoisomerase I. After incubation, the plasmids were deproteinated, agarose-gel-electrophoresed, and stained to observe the topological status. As shown in Fig. 1C, hTFAM induced supercoiling to the relaxed circular DNA dose-dependently until the ratio reached 1 hTFAM/7.5–5.6 bp. Curiously, when the hTFAM concentration increased (≥1 hTFAM/4.5 bp), the supercoiled form proportion decreased sharply (Fig. 1C,D), again indicating substantial changes in the hTFAM–DNA interaction status between the 1 hTFAM/5.6 bp and 1 hTFAM/4.5 bp ratios. Because ethidium bromide (EtBr) intercalates the DNA double helix and induces topological changes, open circular DNA without a nick is transformed into a supercoiled form when electrophoresed in EtBr-containing gels. When plasmids subjected to DNA-unwinding assays were run in EtBr-containing agarose gel, the supercoiled form proportion was similar throughout the reactions (Supplementary Fig. 1B), indicating that no nicking was introduced to plasmid DNA by TFAM addition during DNA-unwinding assays and that, therefore, the sharp decrease in the supercoiled form proportion at higher hTFAM concentrations (≥1 hTFAM/4.5 bp) (Fig. 1C,D) was not caused by plasmid nicking but was genuinely due to the high hTFAM concentration in the reaction. In contrast, when we performed DNA-unwinding assays using *E. coli* topoisomerase I, no supercoiled DNA was formed in the presence of *E. coli* topoisomerase I (Fig. 1E). This was not a consequence of DNA nicking, as the plasmid DNA in Fig. 1E turned into the supercoiled form in EtBr-containing gel (Supplementary Fig. 1C).

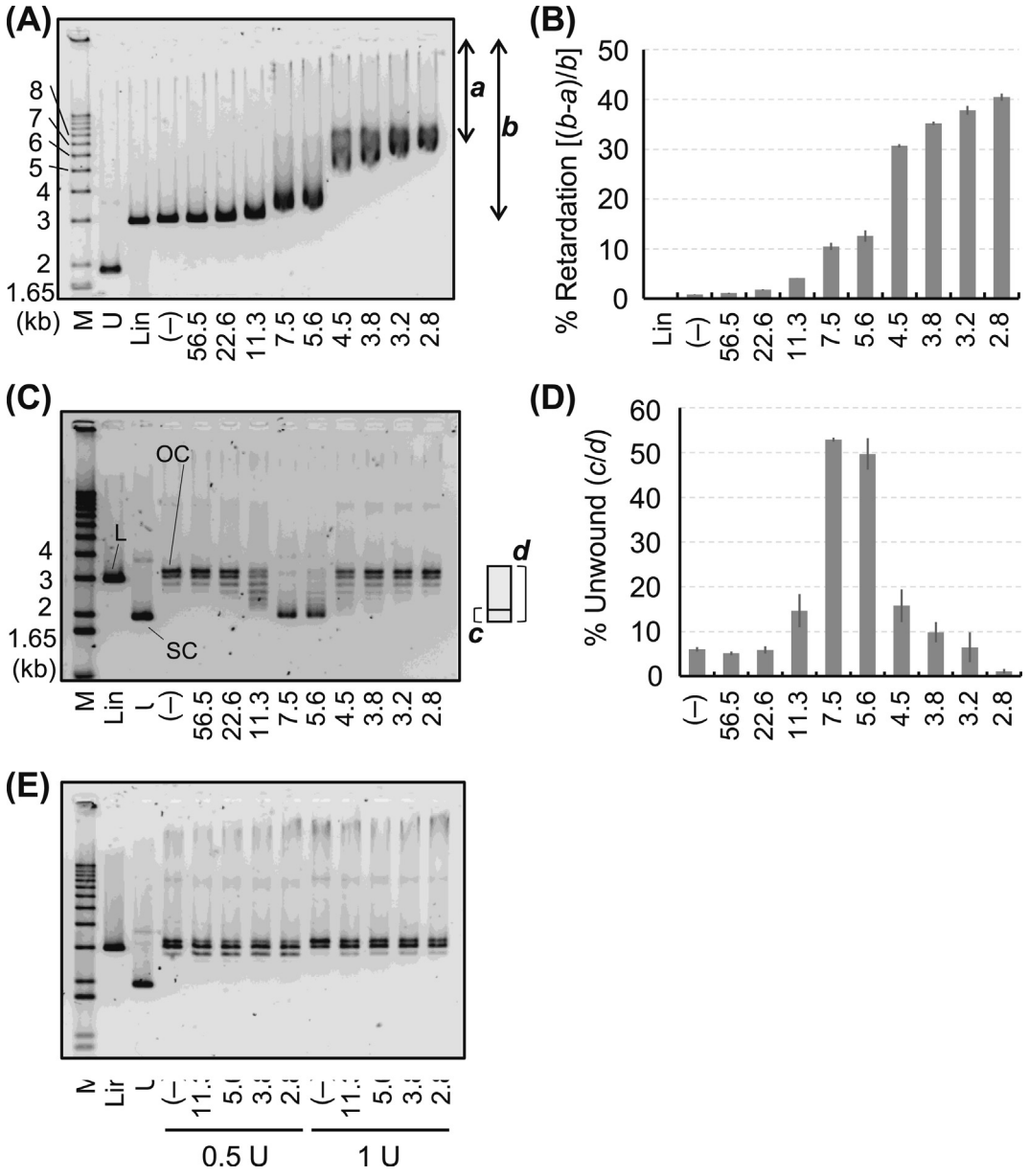

Fig. 1. *In vitro* DNA-binding and DNA-unwinding ability of hTFAM. (A) An electrophoretic mobility shift assay (EMSA) to evaluate DNA-binding ability of hTFAM. A fixed amount of linearized 3 kb plasmid was incubated without (−) or with increasing hTFAM concentrations, and the reaction mixtures were run in agarose gel, followed by Sybr Green I gel staining. The molecular ratios of hTFAM and DNA fragments were 1 hTFAM/56.5, 22.6, 11.3, 7.5, 5.6, 4.5, 3.8, 3.2, and 2.8 bp of DNA fragments. bp values are used to label electrophoretic lanes. Uncut plasmids (U) and linearized plasmids (Lin) with no additional treatment were run in parallel. (B) Evaluation of linearized plasmid retardation by hTFAM binding. *b* is the distance between the well and the linearized plasmid band in the Lin lane in A, and *a* is the distance between the well and the plasmid band in each lane. The extent of retardation in each lane was evaluated by calculating $(b - a)/b$ (%). Data represent the mean of three independent experiments ± SEM. (C) Circular DNA-unwinding by hTFAM. DNA-unwinding ability of hTFAM was analyzed. Plasmids were first relaxed with topoisomerase I, and the relaxed plasmids were incubated without (−) or with increasing hTFAM concentrations in the presence of topoisomerase I. Subsequently, plasmids were extracted and electrophoresed in agarose gel and visualized with Sybr Green I staining. Untreated supercoiled plasmids (U) and linearized plasmids (Lin) with no additional treatment were run in parallel. SC, supercoiled form; L, linear from; OC, open circular form. (D) Evaluation of DNA-unwinding ability of hTFAM. Areas where SC is accumulated and areas covering from SC to OC were defined as areas *c* and *d*, respectively, in each lane in C. Areas *c* approximately include the lowest band and the one above. A schematic drawing of the areas is shown next to the image in C. Densitometric intensities of these areas were measured, and c/d (%) was calculated. Data represent the mean of three independent experiments ± SEM. (E) DNA-unwinding assays with *E. coli* topoisomerase I. Instead of 0.5 unit (U) of calf thymus topoisomerase I, 1 U and 0.5 U of *E. coli* topoisomerase I were used here.

2.2. Chemical acetylation modifies specific lysine residues in hTFAM

To examine how TFAM is nonenzymatically acetylated, we performed chemical acetylation of hTFAM *in vitro*. hTFAM was incubated without (mock-incubation) or with three different acetyl-CoA concentrations under alkaline pH conditions. The first two concentrations (0.1 and 1.5 mM) were selected on the basis of a previous report that estimated mitochondrial acetyl-CoA concentration of 0.1–1.5 mM (Wagner and Payne, 2013), and the third concentration (5 mM) was selected to include the conditions in which a sufficient reaction was likely. An alkaline environment induces deprotonation of the ε-amino group of a lysine residue in a protein. This deprotonated amino group delivers a nucleophilic attack toward the electrophilic carbonyl carbon of the acetyl group in acetyl-CoA, resulting in the acetyl-lysine

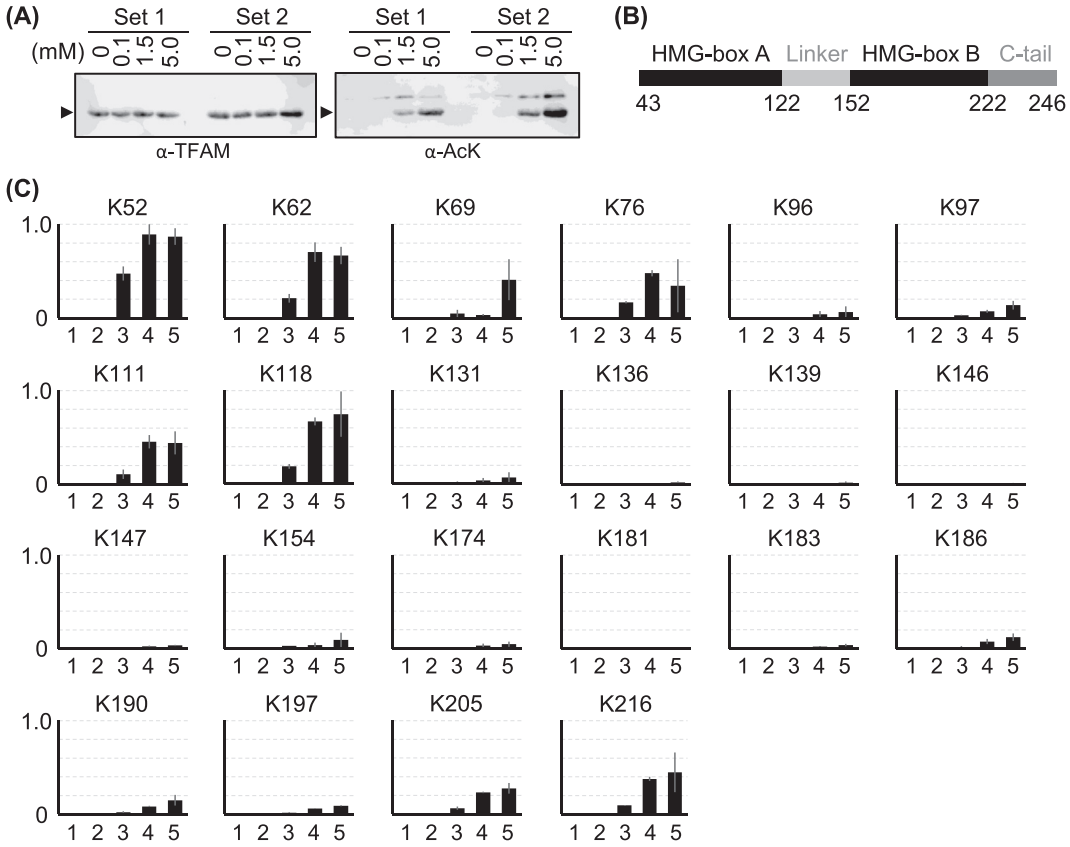

Fig. 2. MS analysis of acetylated hTFAM. (A) Western blotting analysis of the two independently acetylated sample sets for MS analysis. Concentrations of acetyl-CoA used in the *in vitro* incubation (0 for mock incubation, 0.1, 1.5, and 5.0 mM) are indicated. Anti-human TFAM antibodies (α-TFAM) and anti-acetyl-lysine antibodies (α-AcK) were used for hTFAM detection. Bands corresponding to hTFAM are indicated by arrow heads. (B) Mature human TFAM domain structure with amino acid numbers. The mitochondrial targeting sequence (residues 1–42) is not shown. (C) Untreated hTFAM (1), mock-incubated hTFAM (2) and hTFAM treated with 0.1, 1.5, and 5 mM acetyl-CoA (3, 4, and 5, respectively) were subjected to MS analysis to investigate acetylation sites in hTFAM. Two independently processed sample sets were analyzed. The first and second preparation sets were analyzed once and thrice, respectively. Triplicate data of the second set were appropriately averaged, and the mean of the first set data and the averaged second set data is shown as graphs with error of the mean. See details for data processing in Section 4.7 and Supplementary Table 2. The numbers above each graph indicate positions of the detected lysine residues (K) according to unprocessed natural human TFAM sequence with the start codon methionine as 1. Y axis shows normalized intensities (see Section 4.7).

formation (Wagner and Hirschey, 2014). Acetylation incubation was immediately followed by the removal of unreacted acetyl-CoA from the reaction mixtures to avoid uncontrolled acetylation later when protein samples were incubated with an alkaline buffer for trypsin digestion. Western blotting with anti-acetyl-lysine antibodies detected hTFAM treated with acetyl-CoA (Fig. 2A). Untreated hTFAM, mock-incubated hTFAM, and acetyl-CoA-treated hTFAM were digested with trypsin and subjected to mass spectrometry (MS). In acetyl-CoA-treated hTFAM, we observed substantial acetylation at lysine residues K52, K62, K76, K111, and K118, which are located within HMG-box A (Fig. 2B,C and Supplementary Fig. 2). In addition, K216 in HMG-box B appeared to undergo significant acetylation.

2.3. Chemical acetylation decreases the DNA-unwinding ability of hTFAM, but the DNA-binding ability is largely unaffected

Next, we examined the effect of hTFAM acetylation on its DNA-binding and DNA-unwinding ability. hTFAM was incubated with 5 mM acetyl-CoA to introduce nonenzymatic acetylation. Then, buffer exchange was performed to remove unreacted acetyl-CoA. The same procedure was conducted in the absence of acetyl-CoA, and the resulting hTFAM preparation was used as a control. EMSA was performed using acetylated hTFAM (Ac-hTFAM) and mock-incubated hTFAM (Mo-hTFAM) (Fig. 3A). The patterns of gel mobility shift of 3 kb linear DNA by Ac-hTFAM were similar to those by Mo-hTFAM (Fig. 3B–D), indicating that acetylation does not substantially affect the overall DNA-binding ability of hTFAM.

In contrast, DNA-unwinding assays showed a clear difference between Ac-hTFAM and Mo-hTFAM (Fig. 4). While transition of the plasmid topological patterns and hTFAM concentration for maximal unwinding efficiency (1 hTFAM/7.5–5.6 bp) were similar between untreated hTFAM (Fig. 1C,D) and Mo-hTFAM (Fig. 4D,E), approximately 1.5-fold higher Ac-hTFAM concentration was required to achieve maximal unwinding efficiency (1 hTFAM/4.5–3.8 bp) (Fig. 4A,B). In addition, the decrease in DNA-unwinding efficiency with Ac-hTFAM above 1 hTFAM/3.8 bp appeared to be less precipitous compared to that with unmodified hTFAM above 1 hTFAM/5.6 bp (Fig. 4). These results indicated that acetylation significantly decreases TFAM's DNA-unwinding ability in the presence of topoisomerase I, and suggested that acetylation eases an inhibitory effect of the high TFAM concentration on topoisomerase I access to DNA.

3. Discussion

TFAM plays crucial roles in transcription initiation and nucleoid architecture inside the mitochondria of human and other mammals. In transcription initiation, TFAM binds sequence-specifically to the mitochondrial promoters, recruiting mitochondrial RNA polymerase and then mitochondrial transcription factor B2 at transcription start sites to initiate RNA synthesis (Gustafsson et al., 2016). In contrast, nucleoid

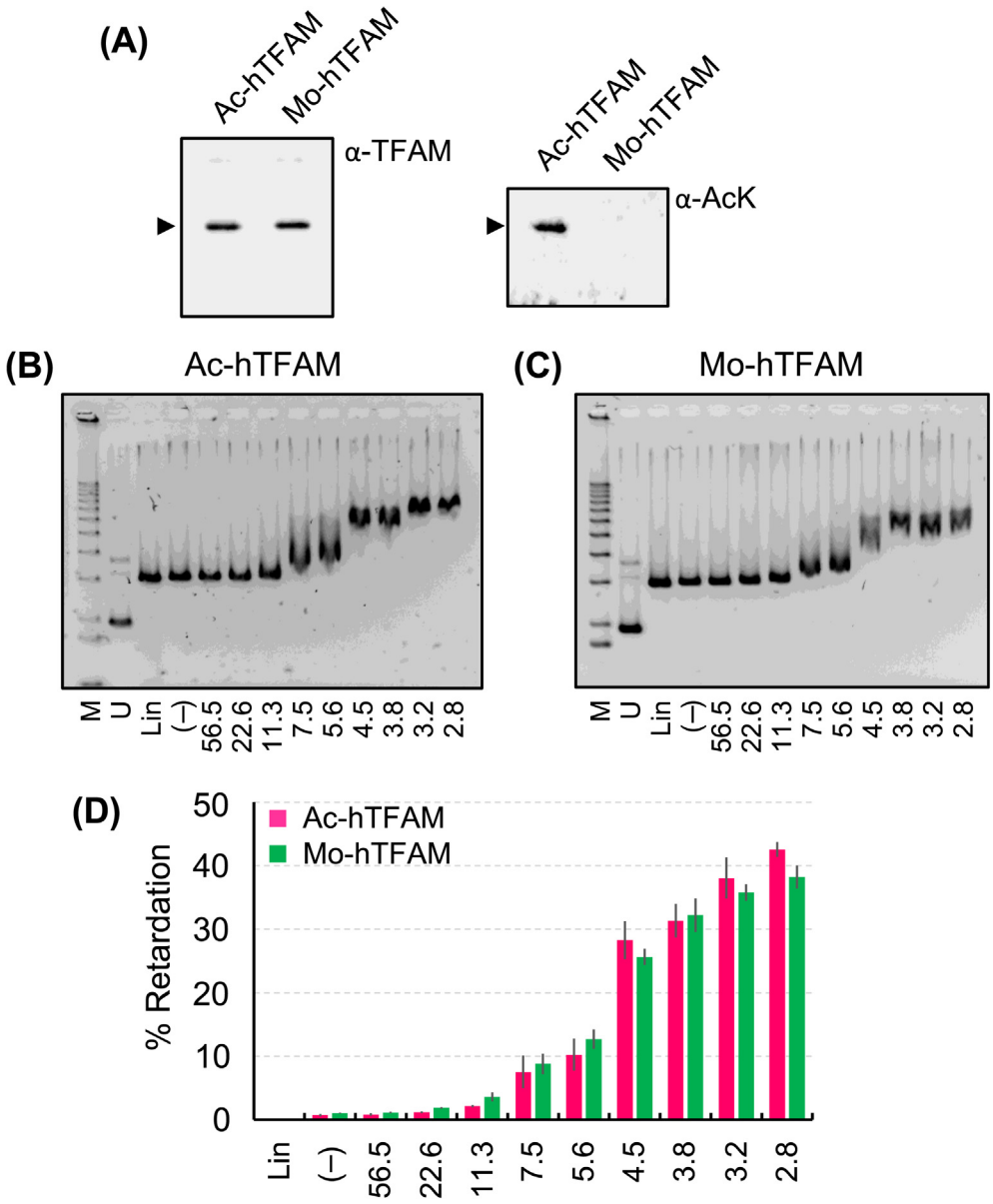

Fig. 3. Evaluation of DNA-binding ability of chemically acetylated hTFAM. (A) Western blotting analysis of hTFAM after chemical acetylation with anti-human TFAM antibodies (α-TFAM) and anti-acetyl-lysine antibodies (α-AcK). Ac-hTFAM, hTFAM treated with 5 mM Acetyl-CoA; Mo-hTFAM, mock-incubated hTFAM. (B–D) EMSAs with Ac-hTFAM and Mo-hTFAM. Experimental procedures and data analyses are similar to those in Fig. 1A,B, and lane labels are as in Fig. 1. Data represent the mean of three independent experiments ± SEM.

architecture involves TFAM's sequence-nonspecific DNA binding and high expression levels that are proposed to be sufficient to coat the entire mitochondrial genome (Farge and Falkenberg, 2019; Kang et al., 2007). Using electron microscopy (EM), Kukat et al. (2015) visualized the relationship between the TFAM–DNA ratio and DNA packaging *in vitro*. They observed induction of DNA packaging at 1 TFAM/30 bp and 1 TFAM/15 bp. When the ratio reached 1 TFAM/6 bp, DNA was shown to be fully packaged (Kukat et al., 2015). Our DNA-unwinding assay results are essentially consistent with the EM observation: at 1 TFAM/22.6–11.3 bp in the reaction mixture, the topology of open circular DNA started changing, and at 1 TFAM/7.5–5.6 bp, DNA unwinding was achieved with maximal efficiently. While no further compaction was observed at higher TFAM concentrations (≥1 TFAM/4.5 bp) in the EM study (Kukat et al., 2015), we detected clear differences in the DNA topological status at 1 TFAM/4.5 bp and above. Our finding can be interpreted that under the conditions of 1 TFAM/7.5–5.6 bp, plasmids sufficiently coated by TFAM are still accessible by topoisomerase I and this enzyme relaxes the TFAM-induced contortion in the DNA double helix, resulting in a dramatic global transition of the circular DNA topology from open circular to supercoiled status. When TFAM was added to the reaction in excess (≥1 TFAM/4.5 bp), topoisomerase I access to DNA was rapidly inhibited and topological modification could be no longer effectively introduced to plasmids, which was coincident with an abrupt upper shift of linear DNA that occurred between 1 TFAM/5.6 bp and 1 TFAM/4.5 bp in EMSA. Excess TFAM loading at ≥1 TFAM/4.5 bp could be assumed to induce a cooperative and therefore rapid change in the TFAM–DNA relationship in DNA-unwinding assays. The apparent consistency of the TFAM–DNA ratio for the full DNA packaging observed by EM (Kukat et al., 2015) and for the maximal unwinding efficiency determined in this study suggests that our *in vitro* assays reasonably and unbiasedly reflect TFAM's sequence-nonspecific function and quantitatively detect TFAM's ability to introduce negative supercoils to bound DNA (see below). The *in vitro* TFAM–DNA ratio for full DNA packaging and maximal unwinding is higher than the ratio of

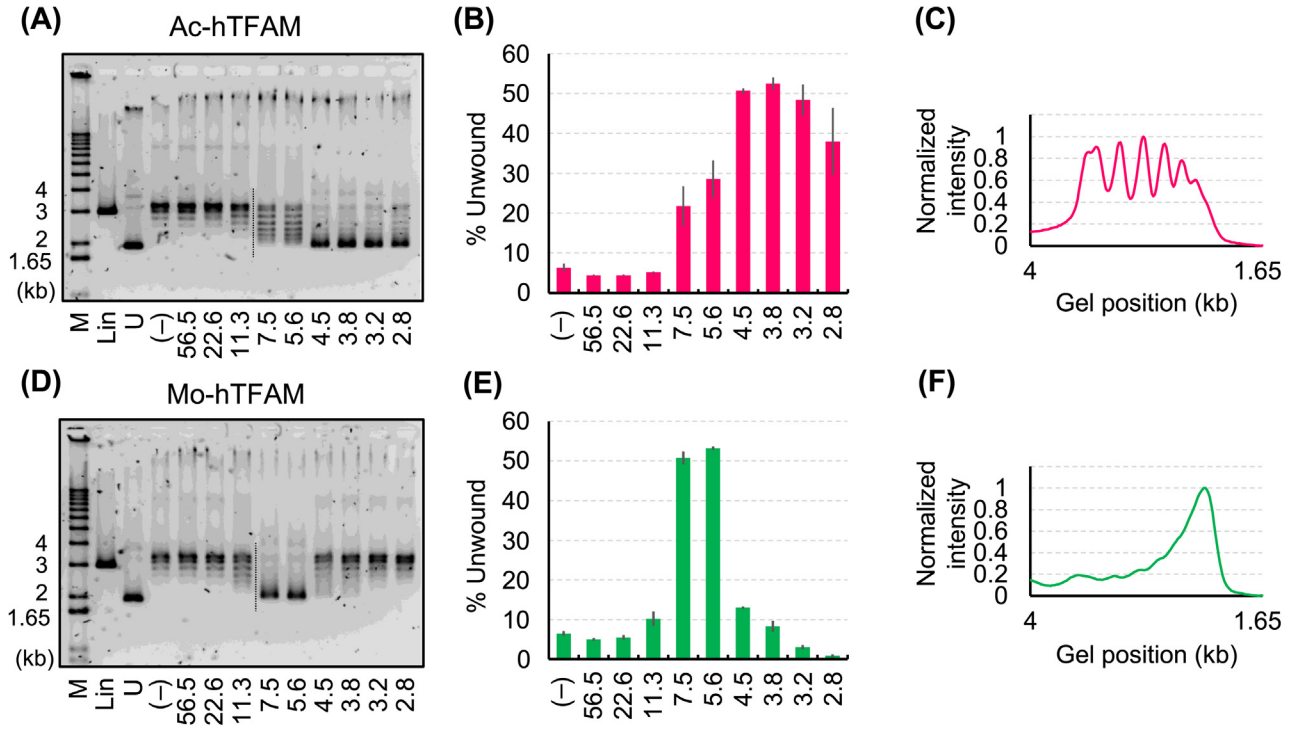

Fig. 4. Evaluation of DNA-unwinding ability of chemically acetylated hTFAM. DNA-unwinding assays were performed with Ac-hTFAM (incubated with 5 mM acetyl-CoA) (A) and Mo-hTFAM (D) in the presence of calf thymus topoisomerase I. (B and E) Quantification of DNA-unwinding assay results were performed as in Fig. 1D. Data represent the mean of three independent experiments ± SEM. (C and F) Densitometric profile of 1 TFAM/7.5 bp lanes in A and D. Analyzed regions of the lanes are indicated as dotted lines in A and D. Y axis is explained in Section 4.3.

TFAM–mtDNA observed in an NP-40-insoluble fraction from human placental mitochondria (1 TFAM per ~18 bp of mtDNA) (Alam et al., 2003) (also see (Takamatsu et al., 2002)). Similar ratio was reported from mouse kidney mitochondria (Ekstrand et al., 2004). It is possible that not all TFAM molecules were associated with DNA in the above *in vitro* experiments and therefore higher TFAM–DNA ratio was required to achieve full DNA packaging and maximal unwinding efficiency.

While eukaryotic topoisomerase I relaxes both negative and positive supercoils, the *E. coli* counterpart relaxes only negative ones (Kornberg and Baker, 1992). The clear difference in the occurrence of plasmid topological changes with the eukaryotic and *E. coli* topoisomerases in our circular DNA-unwinding assay suggests that the TFAM–DNA interaction introduced negative supercoiling within their bound regions, which conversely induced positive supercoiling outside the bound regions, and the positive supercoils could be released only by eukaryotic topoisomerase I. Our interpretation is supported by the fact that native mtDNA is negatively supercoiled when deproteinated and purified from cells (Zhang et al., 2014) and by a crystallographic study in which TFAM-bound DNA was described to be modestly unwound (Rubio-Cosials et al., 2011), and is consistent with an early *in vitro* experiment using chloroquine (Fisher et al., 1992).

Mitochondria are the major acetyl-CoA-producing compartments in most mammals (Pietrocola et al., 2015). Current acetylation research appears to support the idea that nonenzymatic lysine acetylation occurs in mitochondria and contributes to the mitochondrial protein acetylation landscape (Baeza et al., 2016; Hosp et al., 2017; Wagner and Hirschey, 2014). Previous studies reported that TFAM is acetylated in animal tissues and cultured cells (Supplementary Table 1), yet how TFAM acetylation occurs was unclear. Therefore, we investigated the modification mechanism, assuming chemical acetylation as a plausible candidate. We took advantage of *in vitro* acetylation using highly purified recombinant hTFAM and acetyl-CoA and examined acetylation sites by MS. While K52, K62, K76, K111, and K118 in HMG-box A and K216 in HMG-box B showed a significant signature of acetylation, other lysine residues detected appeared only weakly or even not acetylated. Because analysis of numerous sites in several proteins using *in vitro* chemical acetylation assays showed large differences in lysine reactivity with acetyl-CoA (Baeza et al., 2015), our results of the occurrence of highly site-specific modification are not unreasonable. Crucially, four of our identified sites (i.e., K62, K76, K111, and K118) coincide with previously reported sites of acetylation in TFAM from cultured human cells (King et al., 2018). Because the previously analyzed TFAM was transiently overexpressed as a fusion protein with the C-terminus HA tag in cultured human cells (King et al., 2018), endogenous TFAM should share the acetylation sites with its exogenous counterpart. Therefore, the coincidence of many acetylation sites between our *in vitro*-modified hTFAM and the cultured-cell-derived TFAM can be considered data that support that TFAM acetylation occurs nonenzymatically *in vivo*. In addition, the above-mentioned study included TFAM as a substrate and listed K52, K69, K76, K111, and K190 as acetylated sites (Baeza et al., 2015). We found K52, K76, and K 111 to be preferential acetylation sites and K69 and K190 to receive weak acetylation.

Since addition of an acetyl group to a lysine residue eliminates the positive charge of the side chain and increases steric hindrance, acetylation probably significantly changes TFAM activity and/or properties. Therefore, we explored the effects of the modification using acetylated TFAM in EMSA and DNA-unwinding assays. Careful *in vitro* analyses suggested that acetylation affects TFAM's DNA-unwinding ability without reducing its DNA-binding ability. In addition, the inhibitory effect of the excess TFAM in DNA-unwinding assays, likely to be a consequence of inaccessibility of the topoisomerase I to DNA, appears to be alleviated by acetylation. These could be due to possible decreased cooperativity of TFAM as a result of the modification. We infer that when lysine residues in TFAM are acetylated *in vivo*, TFAM binding to mtDNA unlikely deteriorate, maintaining mtDNA stability provided by TFAM binding (Kang et al., 2007). In contrast, TFAM's DNA-unwinding ability significantly decreases as a result of acetylation. This

finding postulates an intriguing idea that TFAM acetylation could change the overall and/or local topology of mtDNA *in vivo*, presumably without compromising mtDNA stability, which could then influence the packaging status and modulate mtDNA gene expression and replication activity.

King et al. (2018) made a recombinant TFAM in which K62, K76, K111, and K118 were all mutated to glutamines. Using sophisticated *in vitro* assays, the authors showed that the DNA-binding affinity of the mutant TFAM was significantly lower than that of the wild-type counterpart and that the requirement of a higher concentration of the mutant compared to the wild type for DNA compaction was due to the reduced binding affinity. We speculate two possibilities for the difference in DNA-binding assay results between King *et al.* and this study. (1) It could be attributed to the intrinsic differences between acetyl-lysine and glutamine residues. Glutamine substitution is often considered an acetyl-lysine mimic owing to the resemblance of uncharged side chains. However, the length and exact chemical structure are different (Supplementary Fig. 3). Therefore, such a "mimic" protein might not necessarily recapitulate the characteristics of the true acetylated counterpart, which is clearly the case with Rtt109, a yeast histone acetyltransferase, which is active in the acetylated form but much less active with glutamine substitution of the acetyl-lysine residue (Albaugh et al., 2011). (2) We used 3 kb DNA fragments and relied on agarose gel electrophoresis in EMSA. Under these conditions, detection of DNA migration retardation should require binding of many TFAM molecules per a DNA fragment. It is possible that our assay did not detect a subtle difference in DNA-binding ability between unmodified and acetylated TFAM.

Of the six lysine residues which we determined to be major acetylation sites (K52, K62, K76, K111, K118, and K216), K52 was shown to have hydrogen-bonded or water-mediated interaction with DNA (Ngo et al., 2011; Ngo et al., 2014). To obtain structural insight into acetylation effects, we examined the four published X-ray crystal structure deposits of TFAM–dsDNA oligonucleotides (pdb IDs: 3TMM, 3TQ6, 4NOD, and 4NNU) (Ngo et al., 2011; Ngo et al., 2014; Rubio-Cosials et al., 2011) (Fig. 5 and Supplementary Fig. 4; also see Supplementary Information). As for K52 and K62, in all analyzed structures except one, nitrogen atoms of ε-amino groups of the lysine residues are located less than 6 Å of their nearest oxygen atoms that are in phosphate groups and are not used for DNA phosphodiester bond formation (Fig. 5A,B). The distance of < 6 Å should allow electrostatic interaction. As for K76, one of the deposits satisfies the above conditions (Supplementary Fig. 4A). In contrast, K216 (and K205) in HMG-box B is not located in the vicinity of such oxygen atoms in DNA backbones (≥ 6 Å) (Supplementary Fig. 4B). Therefore, adding acetyl groups to K52, K62, and K76 could affect the overall HMG-box A–DNA interaction through elimination of positive charges and/or an increase in steric hindrance. TFAM dimerization was observed to be formed through antiparallel interaction of helix 3 in HMG-box A of two TFAM molecules bound to DNA (Ngo et al., 2014). It was proposed that TFAM dimerization contributes to mtDNA packaging (Kaufman et al., 2007; Ngo et al., 2014). Intriguingly, helix 3 contains K111 and K118. However, it is unlikely that K111 and K118 acetylation will directly affect dimerization, because their side chains do not appear to face the interface (Fig. 5C). Collectively, we propose that acetylation at K52, K62, and K76 is mainly responsible for the changes we observed in our *in vitro* assays. Since TFAM interacts with DNA through multiple interactions and contacts (Ngo et al., 2011; Ngo et al., 2014; Rubio-Cosials et al., 2011), it would be reasonable that modification of the three lysine residues does not substantially reduce the overall TFAM binding to DNA but affects the ability to change DNA topology upon binding. In addition, because Dinardo et al. (2003) reported a single acetylation event on rat TFAM, it is possible that not all sites are acetylated at the same time *in vivo*. Simultaneous modification at K52, K62, and K76, and single modification at one of them might have different effect on TFAM property. More experiments are required in order to reveal details of the

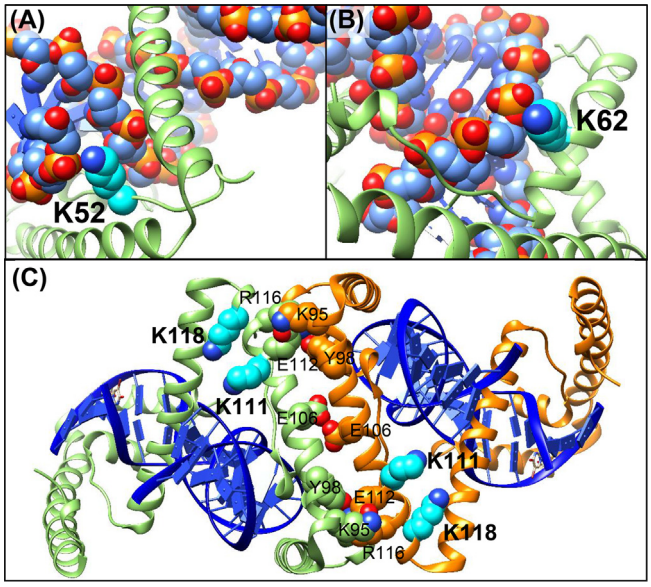

Fig. 5. Structural estimation of TFAM acetylation effects. Acetylation effects were estimated using published crystal structures of TFAM–dsDNA oligonucleotides. (A and B) Close-up views of TFAM/DNA structures surrounding K52 in A (pbd ID: 4NOD) and K62 in B (pbd ID: 3TQ6). TFAM is shown in pale green ribbon presentation. Lysine residues K52 and K62 are highlighted as spheres in A and B, respectively, and their side chains are shown in cyan with nitrogen atoms of ε-amino groups in dark blue. Oxygen, phosphorus, and carbon atoms of DNA backbones are presented as red, orange, and pale-blue spheres, respectively. DNA bases are shown as blue plates. (C) Dimerized TFAM/DNA structure (pbd ID: 4NOD). TFAM molecules are shown in pale green and orange and DNA in blue. K111 and K118 are highlighted as in A. Residues shown to be involved in salt bridges and hydrogen bonds (Ngo et al., 2014) are shown as spheres, with nitrogen and oxygen atoms in blue and red, respectively. See data examination details in Supplementary Information.

acetylation effects on TFAM. It will be also interesting to investigate how TFAM acetylation influences mitochondrial transcription, mtDNA replication, mtDNA topology, and mitochondrial nucleoid formation and segregation.

In mitochondria, acetyl-CoA is generated by various pathways and is generally metabolized in the tricarboxylic acid (TCA) cycle (Pietrocola et al., 2015). Chemical acetylation must be influenced by the acetyl-CoA concentration in mitochondria, and we speculate that under normal conditions, acetyl-CoA might function as a messenger that directly conveys the mitochondrial metabolic status to the mitochondrial genome via TFAM acetylation. On the other hand, under certain nutritional or pathological conditions in which the acetyl-CoA concentration is persistently high, acetyl-CoA could turn into a form of "carbon stress" (Wagner and Hirschey, 2014), which could cause TFAM hyperacetylation, resulting in dysregulation of TFAM function. This would be worthwhile studying, considering the fact that mtDNA encodes subunits for the respiratory chain complexes of the oxidative phosphorylation system that has interplay with the TCA cycle and other metabolic circuitries in mitochondria.

To summarize, this is the first report that investigated the effect of acetylation directly using acetylated TFAM and suggested chemical acetylation as a mechanism of TFAM acetylation experimentally. Further studies are required in order to demonstrate which acetylated lysine residue(s) is responsible for the change in TFAM's DNA-unwinding ability and what the exact roles/consequences of TFAM acetylation are in mtDNA maintenance and expression.

4. Materials and methods

4.1. Expression and purification of recombinant hTFAM

Human TFAM mimicking the mature form fused with the His tag-containing polypeptide at the N-terminus (hTFAM) was recombinantly expressed using a plasmid constructed previously (Ohgaki et al., 2007): DNA fragments containing cDNA of 44–246 amino acid residues of human TFAM are inserted between BamHI and EcoRI sites of pPRO-EX-HTb vector (Invitrogen). The resulting protein was expressed in *E. coli* BL21 cells upon IPTG induction, and the soluble fraction was obtained after cell disruption by sonication. Then, hTFAM was purified sequentially using HisTrap FF crude, HiTrap Heparin HP, and HiLoad 16/600 Superdex 75 pg columns (GE Healthcare Life Sciences) with ÄKTAprime plus (GE Healthcare Life Sciences). Buffers for HisTrap FF crude column chromatography were (i) 50 mM Tris-HCl (pH 7.5), 1 M NaCl, 1 mM 2-mercaptoethanol (2-Me), and 20 mM imidazole (A buffer) and (ii) 50 mM Tris-HCl (pH 7.5), 1 M NaCl, 1 mM 2-Me, and 500 mM imidazole (B buffer). Buffers for HiTrap Heparin HP column chromatography were (i) 50 mM Tris-HCl (pH 7.5), 1 mM EDTA (pH 8.0), 1 mM 2-Me, 2% glycerol, and 500 mM NaCl (A buffer) and (ii) 50 mM Tris-HCl (pH 7.5), 1 mM EDTA (pH 8.0), 1 mM 2-Me, 2% glycerol, and 1.5 M NaCl (B buffer). Buffers for HiLoad 16/600 Superdex 75 pg column chromatography were (i) 10 mM Tris-HCl (pH 7.5), 1 mM EDTA (pH 8.0), 1 mM 2-Me, and 2% glycerol (initialization buffer) and (ii) 10 mM Tris-HCl (pH 7.5), 1 mM EDTA (pH 8.0), 1 mM 2-Me, 2% glycerol, and 1 M NaCl (sample buffer). Purified hTFAM was stored in 1 × PBS/20% glycerol at − 80 °C. Protein concentration was determined using a BCA assay kit (Thermo Fisher Scientific).

4.2. EMSA

The pBluescript ks(−) plasmid (~3 kb) was digested with EcoRV at a single site and used for EMSA. Linearized plasmids (125.5 ng) were incubated without or with 100, 250, 500, 750, 1000, 1250, 1500, 1750, and 2000 ng of hTFAM which give the ratios of 1 hTFAM per 56.5, 22.6, 11.3, 7.5, 5.6, 4.5, 3.8, 3.2, and 2.8 bp of plasmid DNA, respectively, at 37 °C for 30 min in 20 μL reaction mixtures comprising 35 mM Tris-HCl (pH 8.0), 72 mM KCl, 5 mM $MgCl_2$, 5 mM DTT, 5 mM spermidine, 0.1 mg/mL BSA, and 10 mM EDTA. Then, a fraction of the reaction mixtures was electrophoresed in 1% agarose gel without EtBr, and DNA bound by hTFAM was visualized with Sybr Green I staining using an ImageQuant LAS 4000 instrument (GE Healthcare). The images were processed using ImageQuant TL software (GE Healthcare). The extent of hTFAM binding to linearized plasmids was evaluated by the electrophoretic mobility shift (retardation) of DNA migration. One of the three independent DNA-binding assay experiments using Ac-TFAM in Fig. 3 was performed with slightly smaller (~1% less) amounts of Ac-hTFAM.

4.3. DNA-unwinding assay

The ability of hTFAM to change the DNA topology was assessed using a DNA-unwinding assay that was used previously (Ohgaki et al., 2007). 125.5 ng of uncut pBluescript ks(−) plasmid was first treated with 0.5 unit of calf thymus topoisomerase I (TaKaRa) at 37 °C for 30 min in 20 μL reaction mixtures comprising the same components as in EMSA. Then, increasing amounts of hTFAM (0 [mock incubation; (−)], 100, 250, 500, 750, 1000, 1250, 1500, 1750, and 2000 ng) were added to the reaction mixtures, and they were further incubated at 37 °C for 30 min. When using 0.5 or 1 unit of *E. coli* topoisomerase I (New England Biolabs), the reaction mixtures contained 20 mM Tris-HCl (pH 7.5), 50 mM KCl, 20 mM $MgCl_2$, and 0.1 mg/mL BSA. Subsequently, proteinase K was added to the reaction mixtures, and they were incubated at 37 °C for 20 min to degrade proteins, followed by DNA extraction with chloroform:isoamyl alcohol (24:1). Next, a fraction of the recovered plasmid DNA was electrophoresed in 1% agarose gel without EtBr and stained with Sybr Green I. Image visualization and densitometric analyses were performed using an ImageQuant LAS 4000 instrument and ImageQuant TL software. A fraction of the recovered plasmid DNA was again electrophoresed in 1% agarose gel containing 500 ng/mL of EtBr, followed by Southern hybridization using AlkPhos Direct Labelling Reagents (GE Healthcare), and detection of DNA bands and image processing were performed using an ImageQuant LAS 4000 instrument and ImageQuant TL software. A hybridization probe used to detect plasmids was produced with PCR amplification of a region of the pBluescript ks(−) plasmid with the following primer pair: 5′-GAGCG CAGAAGTGGTCCTG-3′ and 5′-ACATTTCCGTGTCGCCCTTATTC-3′. Densitometric image profiling of "7.5 bp" lanes in Fig. 4 was performed using ImageJ software (National Institutes of Health): the obtained raw data (*y* axis data of plot values) for each lane were normalized, with the maximum and minimum plot values of each dataset being 1 and 0, respectively.

4.4. In vitro chemical acetylation

Approximately 18.7 μM hTFAM was incubated with or without acetyl-CoA at 37 °C for 3 h in reaction mixtures comprising 100 mM Hepes-NaOH (pH 8.5), 1 mM EDTA, and different concentrations of acetyl-CoA (0 for mock-incubation, 0.1, 1.5, and 5.0 mM). Then, to remove the unreacted acetyl-CoA from the solution, buffer exchange was performed using 1 × PBS. The reaction mixtures were applied to Vivaspin 500 (Sartorius Stedim Biotech) and centrifuged at 15,000*g* at 20 °C. Then, an appropriate volume of 1 × PBS was added to the remaining solution in the upper unit of the device and centrifugation was performed again. This step was repeated several times until the residual acetylation reaction solution in 1 × PBS was theoretically below 0.1%. Finally, the hTFAM-containing solution was enriched appropriately using the same device, and protein concentration was determined using a BCA assay kit.

4.5. Western blotting

Acetylated hTFAM and mock-incubated hTFAM were subjected to SDS-PAGE, and blotted onto PVDF membranes (Merck Millipore). Western blotting was performed using primary antibodies, an anti-human TFAM antibody (Takamatsu et al., 2002) and an anti-acetyl-lysine antibody (#9441; Cell Signaling Technology). The secondary antibodies used were HRP-conjugates. Protein bands were detected using an ImageQuant LAS 4000 instrument, and the images were processed using ImageQuant TL software.

4.6. Mass spectrometry analysis of acetylated hTFAM

Approximately 10 μg of untreated, mock-incubated or acetylated hTFAM was reduced and denatured in a buffer containing 1% SDS, 2.5 mM Tris(2-carboxyethyl)phosphine hydrochloride, and 100 mM Tris-HCl (pH 7.5) at 65 °C for 10 min. Then, 12.5 mM iodoacetamide was added, and the reaction mixture was incubated at room temperature for 10 min for alkylation. Subsequently, proteins were precipitated with 3 volumes of acetone, and the precipitates were rinsed with 90% acetone and air-dried. Next, the proteins were dissolved in 100 mM triethylammonium bicarbonate buffer and subjected to trypsin digestion at 37 °C overnight. The resultant samples were desalted, evaporated, and resuspended in 20 μL of 0.1% formic acid with 2% (v/v) acetonitrile, and they were then injected into an Easy-nLC 1000 instrument (Thermo Fisher Scientific). Peptides were enriched using a 75 μm × 2 cm trap C18 column (3 μm, 100 Å; Thermo Fisher Scientific) and separated on a 50 μm × 15 cm Acclaim PepMap 100 C18 LC column (2 μm, 100 Å; Thermo Fisher Scientific). The mobile phase comprised 0.1% formic acid in ultrapure water (solvent A) and 0.1% formic acid in acetonitrile (solvent B) and was run at a flow rate of 300 nL/min in a linear gradient of 3%–35% buffer B from 0 to 10 min. The

EASY-nLC 1000 instrument was connected to a Q Exactive Orbitrap mass spectrometer (Thermo Fisher Scientific). Mass spectrometric analysis was performed in data-dependent acquisition mode with full scan (from m/z 350 to m/z 1500 with a resolution of 70,000 at m/z 400; automatic gain control [AGC], 3e6; maximum injection time, 100 ms). For each survey scan, 10 most intense precursor ions were selected for tandem mass spectrometry (MS/MS) and detected at a mass resolution of 17,500 at m/z 400 (normalized collision energy, 27%; AGC, 1e5; maximum injection time, 50 ms).

4.7. Data processing of mass spectrometry data

Raw data obtained from MS analyses were processed using MaxQuant software ver. 1.6.6.0 (http://www.maxquant.org) (Tyanova et al., 2016). MaxQuant uses its own search engine, andromeda, to search directly against the UniprotKB for *Homo sapiens*, including the unprocessed natural human TFAM peptide sequence. Search criteria included a fixed carbamidomethylation on cysteine residue (+57.021 Da), and variable modifications of oxidation on methionine residues (+15.995 Da) and acetylation at the N-terminus of proteins and lysine residues (+42.011 Da). A search was performed against trypsin-digested peptides with the minimum peptide length of six amino acids, allowing a maximum of two missed cleavages. The false discovery rate of proteins and peptides was set at 0.01. Other parameters depended on the default settings in MaxQuant, which are optimized by the developers and are appropriate for most experiments. To evaluate acetylation, we used Acetyl (K)Sites files, which MaxQuant generated from raw MS data of each sample set. For each indicated lysine site (Fig. 2C), fragments in which the indicated lysine residue is acetylated were selected and processed and their accumulative processed intensities were given as “Intensity” in Acetyl (K)Sites files by MaxQuant. We defined the values in “Intensity” columns in each sample set as a dataset, and normalization of each dataset was performed as follows: using the maximum and minimum intensity values (max and min) in a given dataset, the Intensity values (i) in the dataset were expressed using the formula: (i–min)/(max–min). Results are shown in ‘Normalized Intensity’ columns in Supplementary Table 2. Finally, normalized datasets from different MS runs were appropriately averaged and used to estimate the extent of acetylation of the indicated lysine sites. The averaged dataset is presented as graphs in Fig. 2C. Y axis of the graphs shows normalized intensities.

4.8. Comparison of lysine–DNA interactions between reported X-ray crystal structures

Crystal structures of TFAM–dsDNA oligonucleotide complexes (pdb IDs: 3TMM, 3TQ6, 4NNU, and 4NOD) were aligned to each other using the MatchMaker tool in UCSF Chimera program (Pettersen et al., 2004). Side chains of lysine residues K52, K62, K76, K111, K118, K205, and K216 were visualized, and atoms located near nitrogen atoms in ε-amino groups of the lysine residues were examined using the Zone tool and the Distances tool in UCSF Chimera program. Atomic model figures were prepared using UCSF Chimera.

Declaration of Competing Interest

The authors declare that they have no known competing financial interests or personal relationships that could have appeared to influence the work reported in this paper.

Acknowledgements

We thank Dr. Daiki Setoyama for valuable discussion. This work was supported in part by Grants-in-Aid for Scientific Research from the Japan Society for the Promotion of Science [JSPS KAKENHI, Japan grant numbers: 18K06089 to K.M, 17K07504 to T.Y., 17H01550 to K.D.]

Appendix A. Supplementary data

Supplementary data to this article can be found online at https://doi.org/10.1016/j.mito.2020.05.003.

References

Alam, T.I., Kanki, T., Muta, T., Ukaji, K., Abe, Y., Nakayama, H., Takio, K., Hamasaki, N., Kang, D., 2003. Human mitochondrial DNA is packaged with TFAM. Nucleic Acids Res. 31, 1640–1645.
Albaugh, B.N., Arnold, K.M., Lee, S., Denu, J.M., 2011. Autoacetylation of the histone acetyltransferase Rtt109. J. Biol. Chem. 286, 24694–24701.
Baeza, J., Smallegan, M.J., Denu, J.M., 2015. Site-specific reactivity of nonenzymatic lysine acetylation. ACS Chem. Biol. 10, 122–128.
Baeza, J., Smallegan, M.J., Denu, J.M., 2016. Mechanisms and dynamics of protein acetylation in mitochondria. Trends. Biochem. Sci. 41, 231–244.
Casey, J.R., Grinstein, S., Orlowski, J., 2010. Sensors and regulators of intracellular pH. Nat. Rev. Mol. Cell Biol. 11, 50–61.
Chatterjee, A., Seyfferth, J., Lucci, J., Gilsbach, R., Preissl, S., Bottinger, L., Martensson, C.U., Panhale, A., Stehle, T., Kretz, O., Sahyoun, A.H., Avilov, S., Eimer, S., Hein, L., Pfanner, N., Becker, T., Akhtar, A., 2016. MOF acetyl transferase regulates transcription and respiration in mitochondria. Cell 167 722-738 e723.
Choudhary, C., Weinert, B.T., Nishida, Y., Verdin, E., Mann, M., 2014. The growing landscape of lysine acetylation links metabolism and cell signalling. Nat. Rev. Mol. Cell Biol. 15, 536–550.
Dinardo, M.M., Musicco, C., Fracasso, F., Milella, F., Gadaleta, M.N., Gadaleta, G., Cantatore, P., 2003. Acetylation and level of mitochondrial transcription factor A in several organs of young and old rats. Biochem. Biophys. Res. Commun. 301, 187–191.
Ekstrand, M.I., Falkenberg, M., Rantanen, A., Park, C.B., Gaspari, M., Hultenby, K., Rustin, P., Gustafsson, C.M., Larsson, N.G., 2004. Mitochondrial transcription factor A regulates mtDNA copy number in mammals. Hum. Mol. Genet. 13, 935–944.
Fan, J., Shan, C., Kang, H.B., Elf, S., Xie, J., Tucker, M., Gu, T.L., Aguiar, M., Lonning, S., Chen, H., Mohammadi, M., Britton, L.M., Garcia, B.A., Aleckovic, M., Kang, Y., Kaluz, S., Devi, N., Van Meir, E.G., Hitosugi, T., Seo, J.H., Lonial, S., Gaddh, M., Arellano, M., Khoury, H.J., Khuri, F.R., Boggon, T.J., Kang, S., Chen, J., 2014. Tyr phosphorylation of PDP1 toggles recruitment between ACAT1 and SIRT3 to regulate the pyruvate dehydrogenase complex. Mol. Cell 53, 534–548.
Farge, G., Falkenberg, M., 2019. Organization of DNA in mammalian mitochondria. Int. J. Mol. Sci. 20.
Farge, G., Laurens, N., Broekmans, O.D., van den Wildenberg, S.M., Dekker, L.C., Gaspari, M., Gustafsson, C.M., Peterman, E.J., Falkenberg, M., Wuite, G.J., 2012. Protein sliding and DNA denaturation are essential for DNA organization by human mitochondrial transcription factor A. Nat. Commun. 3, 1013.
Farge, G., Mehmedovic, M., Baclayon, M., van den Wildenberg, S.M., Roos, W.H., Gustafsson, C.M., Wuite, G.J., Falkenberg, M., 2014. In vitro-reconstituted nucleoids can block mitochondrial DNA replication and transcription. Cell Rep. 8, 66–74.
Fisher, R.P., Clayton, D.A., 1988. Purification and characterization of human mitochondrial transcription factor 1. Mol. Cell. Biol. 8, 3496–3509.
Fisher, R.P., Lisowsky, T., Parisi, M.A., Clayton, D.A., 1992. DNA wrapping and bending by a mitochondrial high mobility group-like transcriptional activator protein. J. Biol. Chem. 267, 3358–3367.
Gong, F., Miller, K.M., 2013. Mammalian DNA repair: HATs and HDACs make their mark through histone acetylation. Mutat. Res. 750, 23–30.
Gustafsson, C.M., Falkenberg, M., Larsson, N.G., 2016. Maintenance and expression of mammalian mitochondrial DNA. Annu. Rev. Biochem. 85, 133–160.
Hebert, A.S., Dittenhafer-Reed, K.E., Yu, W., Bailey, D.J., Selen, E.S., Boersma, M.D., Carson, J.J., Tonelli, M., Balloon, A.J., Higbee, A.J., Westphall, M.S., Pagliarini, D.J., Prolla, T.A., Assadi-Porter, F., Roy, S., Denu, J.M., Coon, J.J., 2013. Calorie restriction and SIRT3 trigger global reprogramming of the mitochondrial protein acetylome. Mol. Cell 49, 186–199.
Hosp, F., Lassowskat, I., Santoro, V., De Vleesschauwer, D., Fliegner, D., Redestig, H., Mann, M., Christian, S., Hannah, M.A., Finkemeier, I., 2017. Lysine acetylation in mitochondria: From inventory to function. Mitochondrion 33, 58–71.
Kang, D., Kim, S.H., Hamasaki, N., 2007. Mitochondrial transcription factor A (TFAM): roles in maintenance of mtDNA and cellular functions. Mitochondrion 7, 39–44.
Kanki, T., Ohgaki, K., Gaspari, M., Gustafsson, C.M., Fukuoh, A., Sasaki, N., Hamasaki, N., Kang, D., 2004. Architectural role of mitochondrial transcription factor A in maintenance of human mitochondrial DNA. Mol. Cell. Biol. 24, 9823–9834.
Kaufman, B.A., Durisic, N., Mativetsky, J.M., Costantino, S., Hancock, M.A., Grutter, P., Shoubridge, E.A., 2007. The mitochondrial transcription factor TFAM coordinates the assembly of multiple DNA molecules into nucleoid-like structures. Mol. Biol. Cell 18, 3225–3236.
King, G.A., Hashemi Shabestari, M., Taris, K.H., Pandey, A.K., Venkatesh, S., Thilagavathi, J., Singh, K., Krishna Koppisetti, R., Temiakov, D., Roos, W.H., Suzuki, C.K., Wuite, G.J.L., 2018. Acetylation and phosphorylation of human TFAM regulate TFAM-DNA interactions via contrasting mechanisms. Nucleic Acids Res. 46, 3633–3642.
Kornberg, A., Baker, T.A., 1992. DNA Replication, second ed. W.H. Freeman and Co., New York.

Kukat, C., Davies, K.M., Wurm, C.A., Spahr, H., Bonekamp, N.A., Kuhl, I., Joos, F., Polosa, P.L., Park, C.B., Posse, V., Falkenberg, M., Jakobs, S., Kuhlbrandt, W., Larsson, N.G., 2015. Cross-strand binding of TFAM to a single mtDNA molecule forms the mitochondrial nucleoid. Proc. Natl. Acad. Sci. USA 112, 11288–11293.

Kukat, C., Wurm, C.A., Spahr, H., Falkenberg, M., Larsson, N.G., Jakobs, S., 2011. Super-resolution microscopy reveals that mammalian mitochondrial nucleoids have a uniform size and frequently contain a single copy of mtDNA. Proc. Natl. Acad. Sci. USA 108, 13534–13539.

Lu, B., Lee, J., Nie, X., Li, M., Morozov, Y.I., Venkatesh, S., Bogenhagen, D.F., Temiakov, D., Suzuki, C.K., 2013. Phosphorylation of human TFAM in mitochondria impairs DNA binding and promotes degradation by the AAA+ Lon protease. Mol. Cell 49, 121–132.

Matsushima, Y., Goto, Y., Kaguni, L.S., 2010. Mitochondrial Lon protease regulates mitochondrial DNA copy number and transcription by selective degradation of mitochondrial transcription factor A (TFAM). Proc. Natl. Acad. Sci. USA 107, 18410–18415.

Ngo, H.B., Kaiser, J.T., Chan, D.C., 2011. The mitochondrial transcription and packaging factor Tfam imposes a U-turn on mitochondrial DNA. Nat. Struct. Mol. Biol. 18, 1290–1296.

Ngo, H.B., Lovely, G.A., Phillips, R., Chan, D.C., 2014. Distinct structural features of TFAM drive mitochondrial DNA packaging versus transcriptional activation. Nat. Commun. 5, 3077.

Ohgaki, K., Kanki, T., Fukuoh, A., Kurisaki, H., Aoki, Y., Ikeuchi, M., Kim, S.H., Hamasaki, N., Kang, D., 2007. The C-terminal tail of mitochondrial transcription factor a markedly strengthens its general binding to DNA. J. Biochem. 141, 201–211.

Pettersen, E.F., Goddard, T.D., Huang, C.C., Couch, G.S., Greenblatt, D.M., Meng, E.C., Ferrin, T.E., 2004. UCSF Chimera–a visualization system for exploratory research and analysis. J. Comput. Chem. 25, 1605–1612.

Pietrocola, F., Galluzzi, L., Bravo-San Pedro, J.M., Madeo, F., Kroemer, G., 2015. Acetyl coenzyme A: a central metabolite and second messenger. Cell Metab. 21, 805–821.

Pohjoismäki, J.L., Wanrooij, S., Hyvarinen, A.K., Goffart, S., Holt, I.J., Spelbrink, J.N., Jacobs, H.T., 2006. Alterations to the expression level of mitochondrial transcription factor A, TFAM, modify the mode of mitochondrial DNA replication in cultured human cells. Nucleic Acids Res. 34, 5815–5828.

Rubio-Cosials, A., Sidow, J.F., Jimenez-Menendez, N., Fernandez-Millan, P., Montoya, J., Jacobs, H.T., Coll, M., Bernado, P., Sola, M., 2011. Human mitochondrial transcription factor A induces a U-turn structure in the light strand promoter. Nat. Struct. Mol. Biol. 18, 1281–1289.

Scott, I., Wang, L., Wu, K., Thapa, D., Sack, M.N., 2018. GCN5L1/BLOS1 links acetylation, organelle remodeling, and metabolism. Trends. Cell Biol. 28, 346–355.

Scott, I., Webster, B.R., Li, J.H., Sack, M.N., 2012. Identification of a molecular component of the mitochondrial acetyltransferase programme: a novel role for GCN5L1. Biochem. J. 443, 655–661.

Suarez, J., Hu, Y., Makino, A., Fricovsky, E., Wang, H., Dillmann, W.H., 2008. Alterations in mitochondrial function and cytosolic calcium induced by hyperglycemia are restored by mitochondrial transcription factor A in cardiomyocytes. Am. J. Physiol. Cell Physiol. 295, C1561–C1568.

Takamatsu, C., Umeda, S., Ohsato, T., Ohno, T., Abe, Y., Fukuoh, A., Shinagawa, H., Hamasaki, N., Kang, D., 2002. Regulation of mitochondrial D-loops by transcription factor A and single-stranded DNA-binding protein. EMBO Rep. 3, 451–456.

Tyanova, S., Temu, T., Cox, J., 2016. The MaxQuant computational platform for mass spectrometry-based shotgun proteomics. Nat. Protoc. 11, 2301–2319.

Wagner, G.R., Hirschey, M.D., 2014. Nonenzymatic protein acylation as a carbon stress regulated by sirtuin deacylases. Mol. Cell 54, 5–16.

Wagner, G.R., Payne, R.M., 2013. Widespread and enzyme-independent Nepsilon-acetylation and Nepsilon-succinylation of proteins in the chemical conditions of the mitochondrial matrix. J. Biol. Chem. 288, 29036–29045.

Wang, K.Z., Zhu, J., Dagda, R.K., Uechi, G., Cherra 3rd, S.J., Gusdon, A.M., Balasubramani, M., Chu, C.T., 2014. ERK-mediated phosphorylation of TFAM downregulates mitochondrial transcription: implications for Parkinson's disease. Mitochondrion 17, 132–140.

Wang, Y.E., Marinov, G.K., Wold, B.J., Chan, D.C., 2013. Genome-wide analysis reveals coating of the mitochondrial genome by TFAM. PLoS One 8, e74513.

Yasukawa, T., Kang, D., 2018. An overview of mammalian mitochondrial DNA replication mechanisms. J. Biochem. 164, 183–193.

Zhang, H., Zhang, Y.W., Yasukawa, T., Dalla Rosa, I., Khiati, S., Pommier, Y., 2014. Increased negative supercoiling of mtDNA in TOP1mt knockout mice and presence of topoisomerases IIalpha and IIbeta in vertebrate mitochondria. Nucleic Acids Res. 42, 7259–7267.